Molecular Theory for the Viscoelasticity of Compatible Polymer Mixtures. 2. Tube Model with Reptation and Constraint Release Contributions

Chang Dae Han* and Jin Kon Kim

Department of Chemical Engineering and Polymer Research Institute, Polytechnic University, Brooklyn, New York 11201. *Received November 4, 1988; Revised Manuscript Received April 13, 1989*

ABSTRACT: The contribution of constraint release is incorporated into our previous theory to predict the linear viscoelastic properties of compatible polymer mixtures. For this, we used the constraint release mechanism, together with the linear blending law for the relaxation modulus, proposed by Graessley. It has been observed that (1) the predictions of zero-shear viscosity, η_{0b}, with the constraint release parameter $z = 3$, compared favorably with experimental data for binary blends of poly(methyl methacrylate) (PMMA) and poly(vinylidene fluoride) (PVDF) and binary blends of PMMA and poly(styrene-*stat*-acrylonitrile) (PSAN) and (2) the predictions of dynamic storage and loss moduli, $G'_b(\omega)$ and $G''_b(\omega)$, were found to be very sensitive to the polydispersity of the polymer. The theory predicts a linear relationship between the plateau modulus of the blend, G°_{Nb}, and blend composition, whereas experimental evidence suggests that G°_{Nb} versus blend composition plots exhibit *negative* deviations from linearity for both PMMA/PVDF and PMMA/PSAN blend systems. It has been found that the use of a 3.4-power blending law for the relaxation modulus and the tube model, with reptation contribution only, predicts *negative* deviations from linearity in G°_{Nb} versus blend composition plots, consistent with experimental observations.

1. Introduction

In a previous paper[1] we presented a theory that predicts the linear viscoelastic properties of mixtures of two compatible polymers, based on a tube-model approach and a 3.4-power blending law for the stress relaxation modulus. In the development of the theory, only the reptation motion, under an external potential, of two primitive chains with *dissimilar* chemical structures was considered, thus neglecting tube renewal through the release of constraint. It was assumed that the external potential could be represented by a term containing the interaction parameter χ between the two primitive chains with dissimilar chemical structures. The theoretical predictions for zero-shear viscosity and dynamic moduli were found to compare favorably with experimental results for blends of poly(vinylidene fluoride) and poly(methyl methacrylate) and blends of poly(styrene-*stat*-acrylonitrile) and poly(methyl methacrylate).

Earlier, Graessley[2] pointed out that the inclusion of tube renewal through the release of constraint into reptation motion is important in order to accurately predict the effect of polydispersity on the linear viscoelastic properties of entangled polymers. Subsequently, he applied the concept of constraint release to predict the linear viscoelastic properties of binary blends of nearly monodisperse polybutadienes.[3]

Having realized the fact that constraint release would be of great importance in dealing with the reptation motion of two primitive chains, in particular those with *dissimilar* chemical structures, we have now incorporated constraint release into our previous theory in order to predict the linear viscoelastic properties of mixtures of two compatible polymers. In this paper we will present the highlights of this investigation.

2. Theory

The tube model of Doi and Edwards[4] is based on the assumption that there is a tube that can be characterized by a single parameter a, the step length of the tube. This means that the tube model of Doi and Edwards is applicable to polymers having the same chemical structure. However, when there are two primitive chains with *dissimilar* chemical structures, it is reasonable to assume that the chemically dissimilar primitive chains, which are characterized by parameters a_i ($i = 1, 2$), would interact under an external potential, and thus tube reorganization would play an important role in the development of a molecular viscoelastic theory for compatible polymer mixtures.

In a previous paper[1] we assumed that two primitive chains, 1 and 2, with *dissimilar* chemical structures, representing linear, entangled polymers 1 and 2, respectively, reptate in their respective tubes and that, after mixing, the dynamics of the primitive chain 1 can be expressed in the form of the Smoluchowski equation

$$\frac{\partial f_1}{\partial t} = D_1 \frac{\partial^2 f_1}{\partial \xi_1^2} + \frac{\partial}{\partial \xi_1}\left(\frac{D_1}{k_B T}\frac{\partial U}{\partial \xi_1}\right) f_1 \tag{1}$$

where f_1 describes the probability that a segment of chain 1 starting at the origin at $t = 0$ will be found at a position ξ_1 at time t later, D_1 is the curvilinear diffusion constant of chain 1, k_B is the Boltzmann constant, T is the absolute temperature, and U is an external potential. By assuming that $\partial U/\partial \xi_1$ can be expressed in terms of the interaction parameter χ

$$\frac{\partial}{\partial \xi_1}\left(\frac{U}{k_B T}\right) = -\frac{2(-\chi)\phi_2}{a_1} \tag{2}$$

where ϕ_2 is the volume fraction of polymer 2 and a_1 is the tube diameter of chain 1, eq 1 may be rewritten as

$$\frac{\partial f_1}{\partial t} = D_1 \frac{\partial^2 f_1}{\partial \xi_1^2} - \frac{2(-\chi)\phi_2 D_1}{a_1}\frac{\partial f_1}{\partial \xi_1} \tag{3}$$

After solving eq 3 under the appropriate boundary conditions, we obtained the expression[1]

$$F_1(t) = \frac{4}{\pi^2}\sum_{p=1}^{\infty}\frac{H_{1,p}}{p^2}\exp(-p^2 t/\tau_{1,p}) \tag{4}$$

where $F_1(t)$ describes the fraction of segments in chain 1 at time t, which are still in tube 1 defined at time $t = 0$ (the original tube). Similarly, the dynamics for chain 2 representing polymer 2 is given by

$$F_2(t) = \frac{4}{\pi^2}\sum_{p=1}^{\infty}\frac{H_{2,p}}{p^2}\exp(-p^2 t/\tau_{2,p}) \tag{5}$$

where $\tau_{i,p}$ ($i = 1, 2$) in eq 4 and 5 are defined by

0024-9297/89/2222-4292$01.50/0 © 1989 American Chemical Society

$$\tau_{i,p} = \tau_{di} \Big/ \left[1 + \left(\frac{(-\chi)\phi^*_i Z_i}{p\pi}\right)^2\right] \tag{6}$$

whee $\phi^*_1 = \phi_2$, $\phi^*_2 = \phi_1$, Z_i is the number of segments in chain i, and $\tau_{di} = L_i^2/D_i\pi^2$ is the tube disengagement time for chain i, in which L_i is the curvilinear contour length and D_i is the diffusion constant for chain i. $H_{i,p}$ (i = 1, 2) in eq 4 and 5 are defined by

$$H_{i,p} = \frac{\{1 - (-1)^p \cosh [(-\chi)\phi^*_i Z_i]\}}{\{1 + [(-\chi)\phi^*_i Z_i/p\pi]^2\}^2} \tag{7}$$

In introducing the contribution of constraint release to the reptation motion of a binary mixture of linear, entangled monodisperse homopolymers having *dissimilar* chemical structures, we will adopt an approach similar to that taken by Graessley and Struglinski[3] who considered the linear viscoelastic properties of a binary mixture of monodisperse homopolymers with *identical* chemical structure. It should be mentioned that the primary purpose of their study was to investigate the effect of polydispersity on the linear viscoelastic properties of a homopolymer.

We now assume that the relaxation modulus of the binary mixture $G_b(t)$ under consideration is represented by

$$G_b(t) = G^\circ_{N1} w_1 F_1(t) R_1(t) + G^\circ_{N2} w_2 F_2(t) R_2(t) \tag{8}$$

where G°_{Ni} (i = 1, 2) are the plateau moduli, w_i (i = 1, 2) are the weight (or volume) fractions, R_i (i = 1, 2) are the reduced relaxation functions, $F_1(t)$ is given by eq 4, and $F_2(t)$ is given by eq 5. Note that R_i (i = 1, 2) is associated with constraint release and defined by[2]

$$R_i(t) = \frac{1}{Z_i}\sum_{j=1}^{Z_i} \exp[-\lambda_{j,i} t/2\tau_w] \qquad i = 1, 2 \tag{9}$$

where the $\lambda_{j,i}$ is defined by

$$\lambda_{j,i} = 4 \sin^2 [\pi j/2(Z_i + 1)] \qquad i = 1, 2 \tag{10}$$

and τ_w is the waiting time that governs the time scale of tube renewal and is defined by[2]

$$\tau_w = \int_0^\infty [w_1 F_1(t) + w_2 F_2(t)]^z \, dt \tag{11}$$

where z is a constraint release parameter, which governs the strength of the constraint release contribution. At the present time, there does not exist any rigorous guideline for choosing a value of z, and thus z can be regarded as an adjustable parameter.

For binary blends, analytical expressions for τ_w can be obtained from eq 11 for any integer value of z. For z = 3, for instance, which was chosen by Graessley and Struglinski,[3] substituting eq 4 and 5 into eq 11 and integrating the resulting expression, one obtains

$$\tau_w = \left(\frac{4}{\pi^2}\right)^3 \left\{\sum_i^\infty \sum_j^\infty \sum_k^\infty \left[\left(\frac{H_{1,i}}{i^2}\right)\left(\frac{H_{1,j}}{j^2}\right)\left(\frac{H_{1,k}}{k^2}\right) \times \frac{{w_1}^3 \tau_{d1}}{i^2 Q_{1,i} + j^2 Q_{1,j} + k^2 Q_{1,k}} + \left(\frac{H_{1,i}}{i^2}\right)\left(\frac{H_{1,j}}{j^2}\right)\left(\frac{H_{2,k}}{k^2}\right) \frac{3 w_1^2 w_2 \tau_{d1} \tau_{d2}}{\tau_{d2}(i^2 Q_{1,i} + j^2 Q_{1,j}) + \tau_{d1} k^2 Q_{2,k}} + \left(\frac{H_{1,i}}{i^2}\right)\left(\frac{H_{2,j}}{j^2}\right)\left(\frac{H_{2,k}}{k^2}\right) \frac{3 w_1 w_2^2 \tau_{d1} \tau_{d2}}{\tau_{d2} i^2 Q_{1,i} + \tau_{d1}(j^2 Q_{2,j} + k^2 Q_{2,k})} + \left(\frac{H_{2,i}}{i^2}\right)\left(\frac{H_{2,j}}{j^2}\right)\left(\frac{H_{2,k}}{k^2}\right) \frac{{w_2}^3 \tau_{d2}}{i^2 Q_{2,i} + j^2 Q_{2,j} + k^2 Q_{2,k}}\right]\right\} \tag{12}$$

where

$$Q_{m,n} = 1 + [(-\chi)\phi^*_m Z_m/\pi n]^2 \qquad m = 1, 2 \tag{13}$$

and $H_{m,n}$ (m = 1, 2) is given by eq 7. Note that, for χ = 0, eq 12 reduces to the same expression as that given in Appendix B of ref 5, where blends of binary components with *identical* chemical structure were considered.

Since the relaxation modulus $G_b(t)$ is given by eq 8, we can obtain the zero-shear viscosity, η_{ob}, steady-state compliance, J°_{eb}, dynamic storage modulus, $G'_b(\omega)$, and dynamic loss modulus, $G''_b(\omega)$, as

$$\eta_{ob} = \frac{4}{\pi^2}\sum_{i=1}^2 w_i G^\circ_{Ni} \left\{\sum_{p=1}^\infty \frac{H_{i,p}}{p^2} \frac{1}{Z_i} \sum_{j=1}^{Z_i} \tau_{i,j}\right\} \tag{14}$$

$$J^\circ_{eb} = \left(\frac{4}{\pi^2}\sum_{i=1}^2 w_i G^\circ_{Ni} \left\{\sum_{p=1}^\infty \frac{H_{i,p}}{p^2} \frac{1}{Z_i} \sum_{j=1}^{Z_i} (\tau_{i,j})^2\right\}\right) \Big/ {\eta_{ob}}^2 \tag{15}$$

$$G'_b(\omega) = \frac{4}{\pi^2}\sum_{i=1}^2 w_i G^\circ_{Ni} \left\{\sum_{p=1}^\infty \frac{H_{i,p}}{p^2} \frac{1}{Z_i} \sum_{j=1}^{Z_i} \frac{(\omega\tau_{i,j})^2}{1 + (\omega\tau_{i,j})^2}\right\} \tag{16}$$

$$G''_b(\omega) = \frac{4}{\pi^2}\sum_{i=1}^2 w_i G^\circ_{Ni} \left\{\sum_{p=1}^\infty \frac{H_{i,p}}{p^2} \frac{1}{Z_i} \sum_{j=1}^{Z_i} \frac{\omega\tau_{i,j}}{1 + (\omega\tau_{i,j})^2}\right\} \tag{17}$$

where

$$\frac{1}{\tau_{i,j}} = \frac{p^2}{\tau_{i,p}} + \frac{\lambda_{j,i}}{2\tau_w} \tag{18}$$

in which $\tau_{i,p}$ is defined by eq 6, $H_{i,p}$ by eq 7, $\lambda_{j,i}$ by eq 10, and τ_w by eq 11. It can be shown that eq 14 reduces to eq 26 of ref 3 and that eq 15 reduces to eq 27 of ref 3, for the following special conditions: (1) large values of Z_i (say, $Z_i > 20$); (2) χ = 0; and (3) $G^\circ_{N1} = G^\circ_{N2} = G^\circ_N$, i.e., for binary mixtures having components with *identical* chemical structure.[6]

Since information on the tube disengagement times τ_{di} (i = 1, 2) are, in general, difficult to obtain, while the viscosities η_{oi} (i = 1, 2) of the constituent components are readily measured, it is of practical importance to express the viscosity of the blends η_{ob} in terms of η_{oi} (i = 1, 2). Using eq 14, we can relate τ_{di} to η_{oi} by

$$\tau_{di} = \left(\frac{\eta_{oi}}{G^\circ_{Ni}}\right) \Big/ \left\{\frac{8}{\pi^2}\sum_{\substack{p \\ \text{odd}}}^\infty \frac{1}{p^2} \frac{1}{Z_i} \sum_{j=1}^{Z_i} \frac{1}{p^2 + (\lambda_{j,i}/2\Lambda)}\right\} \tag{19}$$

where Λ is defined by[2]

$$\Lambda = \left(\frac{8}{\pi^2}\right)^z \sum_{\substack{i \\ \text{all}}}^\infty \sum_{\substack{j \\ \text{all}}}^\infty \sum_{\substack{k \\ \text{odd}}}^\infty \cdots \sum_z^\infty \left(\frac{1}{i^2 j^2 k^2 \ldots z^2}\right)\left(\frac{1}{i^2 + j^2 + \ldots + z^2}\right) \tag{20}$$

which can be approximated by[2]

$$\Lambda = \frac{1}{z}\left(\frac{\pi^2}{12}\right)^z \tag{21}$$

By substituting eq 19 into eq 14, with the aid of eq 18, we obtain

$$\eta_{ob} = \sum_{i=1}^2 \left[\frac{w_i \eta_{oi} \sum_{p=1}^\infty \frac{H_{i,p}}{p^2} \frac{1}{Z_i} \sum_{j=1}^{Z_i} \frac{1}{p^2 Q_{i,p} + \lambda_{j,i}(\tau_{di}/2\tau_w)}}{2\sum_{\substack{p \\ \text{odd}}}^\infty \frac{1}{p^2} \frac{1}{Z_i} \sum_{j=1}^{Z_i} \frac{1}{p^2 + (\lambda_{j,i}/2\Lambda)}}\right] \tag{22}$$

where $H_{i,p}$ and $Q_{i,p}$ are given by eq 7 and 13, respectively, and τ_w is defined by eq 12.

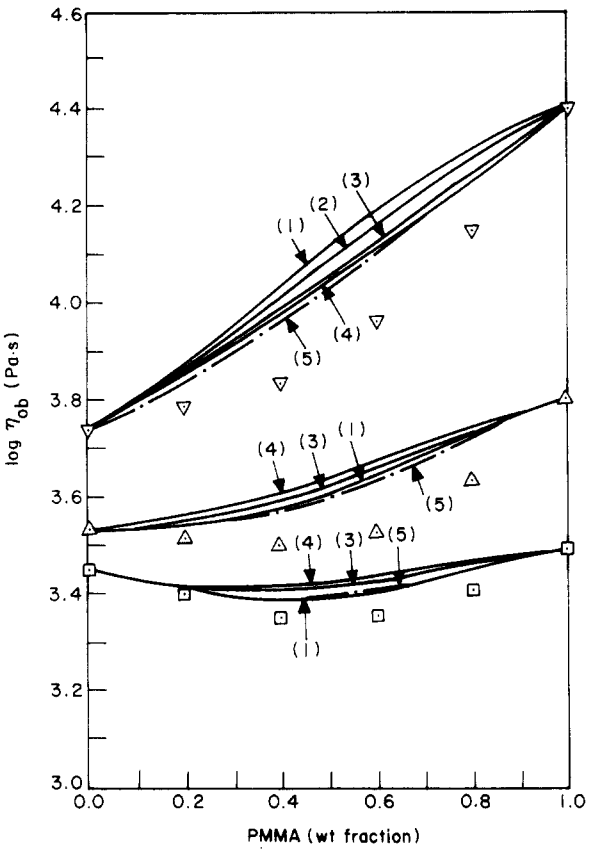

Figure 1. Comparison of theoretical predictions with experimental results for the dependence of log η_{ob} on blend composition for PMMA/PVDF blends with $\chi = -0.3$, at three different temperatures. Curve (1) is predicted with eq 22, for $z = 0$; curve (2) is predicted with eq 22, with $z = 1$; curve (3) is predicted with eq 22, for $z = 3$; curve (4) is predicted with eq 22, for $z = 6$; for $z = 6$; curve (5) is predicted with the 3.4-power blending law together with the reptation contribution only, in the tube model (eq 17 of ref 1). Symbols represent experimental data[1] at different temperatures (°C): (▽) 200; (△) 220; (□) 230.

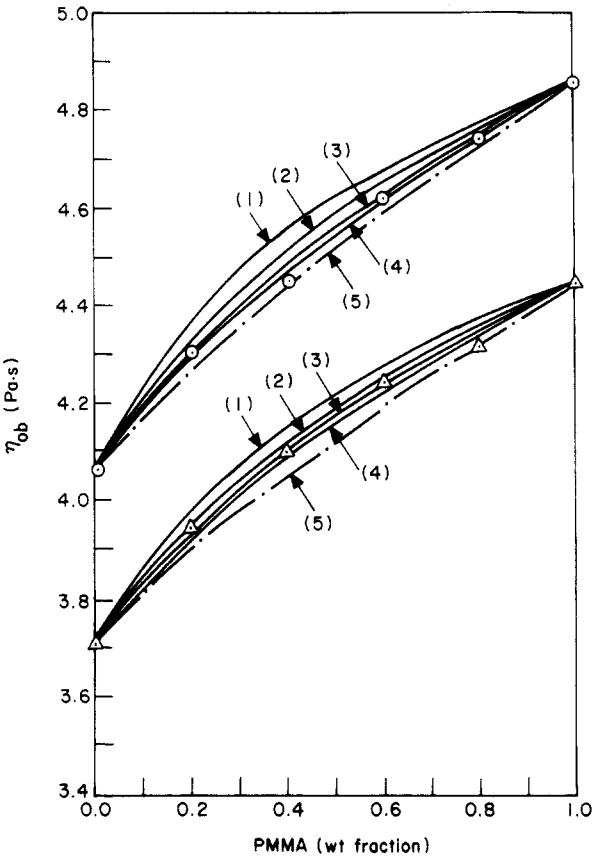

Figure 2. Comparison of theoretical predictions with experimental results for the dependence of log η_{ob} on blend composition for PMMA/PSAN blends with $\chi = -0.01$, at two different temperatures. Curve (1) is predicted with eq 22, for $z = 0$; curve (2) is predicted with eq 22, for $z = 1$; curve (3) is predicted with eq 22, for $z = 3$; curve (4) is predicted with eq 22, for $z = 6$; curve (5) is predicted with the 3.4-power blending law together with the reptation contribution only, in the tube model (eq 17 of ref 1). Symbols represent experimental data[1] at different temperatures (°C): (⊙) 200; (▲) 210.

3. Results and Discussion

In assessing the predictability of the theory presented above, we considered the same blend systems as those considered in our previous paper,[1] namely, binary blends of poly(vinylidene fluoride) (PVDF) and poly(methyl methacrylate) (PMMA) and binary blends of poly(methyl methacrylate) (PMMA) and poly(styrene-*stat*-acrylonitrile) (PSAN). In the computations, we used the same numerical values of the various molecular parameters as were used in our previous paper,[1] specifically: (1) for the PMMA/PVDF mixtures, (i) $M_1 = 7.92 \times 10^4$ for PMMA and $M_2 = 1.45 \times 10^5$ for PVDF; (ii) $G°_{N1} = 6.0 \times 10^5$ Pa for PMMA and $G°_{N2} = 4.0 \times 10^5$ Pa for PVDF; (iii) $Z_1 = 13.8$ for PMMA and $Z_2 = 12.2$ for PVDF; and (2) for the PMMA/PSAN mixtures, (i) $M_1 = 1.05 \times 10^5$ for PMMA and $M_2 = 1.50 \times 10^5$ for PSAN; (ii) $G°_{N1} = 6.0 \times 10^5$ Pa for PMMA and $G°_{N2} = 2.28 \times 10^5$ Pa for PSAN; (iii) $Z_1 = 18.8$ for PMMA and $Z_2 = 10.3$ for PSAN.

We have calculated η_{ob} for different blend compositions, using eq 22 with different values of z, and the results are given in Figure 1 for the PMMA/PVDF blends at 200, 220, and 230 °C with $\chi = -0.3$ and in Figure 2 for the PMMA/PSAN blends at 200 and 210 °C with $\chi = -0.01$. Nishi and Wang[7] reported $\chi = -0.295$ for PMMA/PVDF blends, and Schmitt et al.[8] reported $\chi = -0.011$ for PMMA/PSAN blends. Symbols in Figures 1 and 2 represent the experimental data reported in our previous paper.[1] It should be mentioned that, in using eq 22 to calculate the zero-shear viscosity of the blends, η_{ob}, which is presented in Figures 1 and 2, we used experimental values of η_{o1} and η_{o2}. Since the molecular weights of the constituent components, i.e., PMMA and PVDF in the PMMA/PVDF blends and PMMA and PSAN in the PMMA/PSAN blends, are greater than the entanglement molecular weights of the respective components, the use of the experimentally determined values of η_{o1} and η_{o2} implies that we have used an empirical relationship, $\eta_o \propto M^{3.4}$, instead of the reptation theory, which predicts $\eta_o \propto M^3$.

In reference to Figures 1 and 2, it should be mentioned that the predictions for $z = 0$ represent the tube model with reptation contribution only, together with the linear blending law. At present, there is no theoretical basis for the choice of the value of z. In their study of linear viscoelastic properties of binary blends of nearly monodisperse polybutadienes, Graessley and Struglinski[3] found that the value of $z = 3$ gave the best fit to their experimental data. It can be seen in Figures 1 and 2 that the differences between the predicted values of η_{ob} for $z = 3$ and those for $z = 6$ can be regarded as being very small for all intents and purposes. Nevertheless, at present, z must be regarded as an adjustable parameter. It should be mentioned that the computational time required increases very rapidly as the value of z increases from 3 to 6 for large values of p, and in this study we carried out computations for η_{ob} with p up to 100 for $z = 3$ and p up to 25 for $z = 6$. Very recently, Composto,[9] who investigated mutual diffusion of polystyrene and poly(2,6-dimethyl-

1,4-phenylene oxide), also considered both the reptation and constraint release contributions and concluded that values of z up to about 19 were needed to explain his experimental results.

For comparison purposes, the predicted values of η_{ob} with the 3.4-power blending law and with reptation contribution only, reported in our previous paper,[1] are also given in Figures 1 and 2. The following observations are worth noting in Figures 1 and 2.

For the PMMA/PVDF blend system, the theory predicts that log η_{ob} goes through a minimum at a certain blend composition at 230 °C and shows *negative* deviations from linearity at 220 and 200 °C. Note in Figure 1 that the viscosity ratio η_o(PMMA)/η_o(PVDF) decreases with increasing temperature, and thus it appears that the existence of a minimum in log η_{ob} versus blend composition plots, observed in Figure 1, depends on the value of η_o(PMMA)/η_o(PVDF). Figure 1 shows further that for large values of η_o(PMMA)/η_o(PVDF) the predictions of η_{ob} with the 3.4-power blending law and with reptation contribution only in the tube model are slightly better than those with the linear blending law and with both reptation and constraint release contributions for $z = 3$, but for small values of η_o(PMMA)/η_o(PVDF) the differences between the two predictions are virtually constant. For the PMMA/PSAN blend system shown in Figure 2, the theory predicts that log η_{ob} shows *positive* deviations from linearity. It should be mentioned that the theoretical predictions of *positive* deviations of η_{ob} from linearity for the PMMA/PSAN blend sytem are due to the very small value of $-\chi$ for the PMMA/PSAN pair. Figure 2 shows further that the predictions of η_{ob} with the linear blending law and with both reptation and constraint release contributions for $z = 3$ are slightly better than those with the 3.4-power blending law and with reptation contribution only.

It is of interest to note in Figures 1 and 2 that our theory predicts reasonably well the composition dependence of zero-shear viscosity for the PMMA/PSAN blend system but rather poorly for the PMMA/PVDF blend system, especially at 200 °C. We believe that there are, among others, two primary reasons for the disagreements observed for the PMMA/PVDF blend system, namely, (1) uncertainties involved in the temperature dependence of the interaction parameter χ for the PMMA/PVDF pair and (2) large differences in the temperature dependence of viscosity between PMMA and PVDF.

Since the absolute value of χ decreases with increasing temperature for blends exhibiting a lower critical solution temperature (LCST), it is reasonable to expect that, for the PMMA/PVDF blend system, which exhibits an LCST, the absolute value of χ would be greater, for instance, at 200 °C than at 220 °C. Thus, if a value of $\chi = -0.5$, instead of $\chi = -0.3$, is assigned at 200 °C, the theoretical predictions given in Figure 1 will be improved considerably (see Figure 1 of ref 1). This argument is presented here to merely point out an urgent need for information on the temperature dependence of χ for PMMA/PVDF blends, in order to be able to assess the accuracy (or the lack of accuracy) of the theoretical predictions presented in this paper.

In order to demonstrate differences in the temperature dependence of viscosity between PMMA and PVDF, plots of log a_T versus temperature are given in Figure 3, where a_T is a viscosity shift factor. For comparison purposes, similar plots are given in Figure 4 for PMMA and PSAN. It can be seen in Figures 3 and 4 that there are large differences in the values of a_T between PMMA and PVDF but very little difference in the values of a_T between

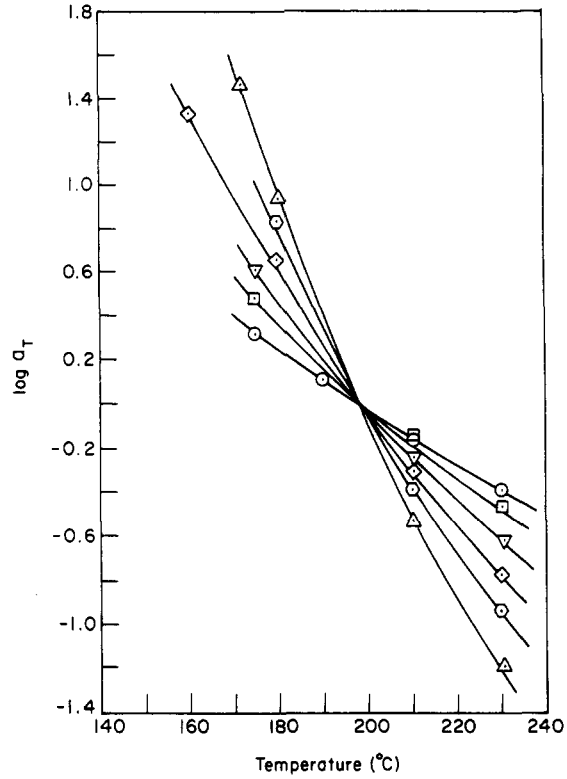

Figure 3. log a_T versus temperature for PMMA/PVDF blends: (▲) PMMA; (⊙) PVDF; (⊡) PMMA/PVDF = 20/80; (▼) PMMA/PVDF = 40/80; (◈) PMMA/PVDF = 60/40; (◎) PMMA/PVDF = 80/20. The reference temperature used is 200 °C.

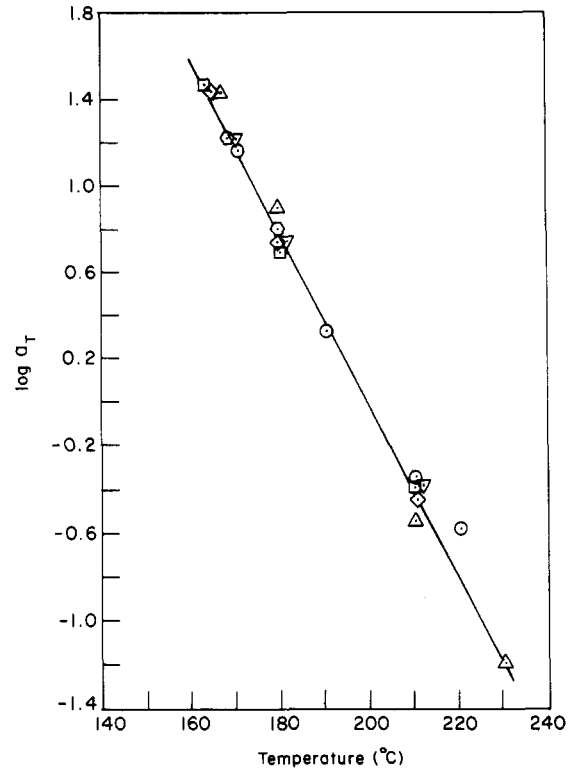

Figure 4. log a_T versus temperature for PMMA/PSAN blends: (▲) PMMA; (⊙) PSAN; (⊡) PMMA/PSAN = 20/80; (▼) PMMA/PSAN = 40/60; (◈) PMMA/PSAN = 60/40; (◎) PMMA/PSAN = 80/20. The reference temperature used is 200 °C.

PMMA and PSAN. The above observation seems to suggest that the rather poor theoretical predictions given in Figure 1, especially at 200 °C, may in part be attrib-

utable to the large differences in the temperature dependence of viscosity between PMMA and PVDF. If this is the case, the relative temperature dependences of the dynamics may play a greater role than the thermodynamics of mixing and the topology of the blend system. This subject is worth investigating in the future by modifying the present theory.

Earlier, Montfort et al.[10] considered constraint release to predict the viscoelastic behavior of binary blends having components with *identical* chemical structure and predicted that plots of η_{ob} versus blend composition on *logarithmic* coordinates for such blends exhibit sigmoidal curvature. But, when η_{ob} is plotted against blend composition on *semilogarithmic* coordinates (i.e., log η_{ob} versus blend composition plots), Montfort's prediction shows *positive* deviations from linearity. Note that this can be predicted as a special case ($\chi = 0$ and $G^\circ_{N1} = G^\circ_{N2} = G^\circ_N$) of the present theory. It is of interest to mention at this juncture that a recent experimental study by Struglinski and Graessley[11] shows that plots of log η_o versus blend composition for binary blends of nearly monodisperse polybutadienes exhibit *positive* deviations from linearity. It should be noted, however, that it is *not* possible to extend the predictions made by Montfort et al. for binary blends having components with *identical* chemical structure to predictions of viscoelastic properties of binary blends having components with *dissimilar* chemical structures.

It should be pointed out that the linear blending law introduced in this paper has the following advantage over the 3.4-power blending law used in our previous paper;[1] namely, the linear blending law enables us to obtain *exact* analytical expressions for η_{ob}, $G'_b(\omega)$, and $G''_b(\omega)$, satisfying Kramers–Kronig's relations[12] for any integer value of the constraint release parameter z, whereas the 3.4-power blending law does not allow us to obtain analytical expressions and the *approximate* analytical solutions so obtained do not satisfy Kramers–Kronig's relations.

For large values of Z_i, eq 19 reduces to

$$\tau_{di} = \left(\frac{\eta_{oi}}{G^\circ_{Ni}}\right) \Bigg/ \left\{\frac{8}{\pi^2}\sum_{p\ \mathrm{odd}}^{\infty}\frac{1}{p^3}\frac{1}{[p^2 + 2/\Lambda]^{1/2}}\right\} \quad (23)$$

For $z = 3$, substitution of eq 21 in eq 23 gives

$$\tau_{di} = \left(\frac{\eta_{oi}}{G^\circ_{Ni}}\right) \Big/ 0.244 \quad (24)$$

On the other hand, the numerical value for the denominator of eq 19 is 0.237 for PMMA having $Z_1 = 13.8$ and 0.236 for PVDF having $Z_2 = 12.2$. These values are close to 0.244, which was determined from the denominator of eq 23. Note further that when only reptation motion is considered in the tube model, we have[4]

$$\tau_{di} = \left(\frac{\eta_{oi}}{G^\circ_{Ni}}\right) \Big/ 0.822 \quad (25)$$

Thus, a comparison of eq 24 and 25 reveals that, for the PMMA/PVDF blends under consideration, the value of τ_{di} for both reptation and constraint release contributions is about 3.4 times that for reptation contribution only. It should be remembered that τ_{di} depends on the number of segments Z_i when constraint release is included in the tube model.

Figure 5 gives plots of theoretical predictions for the *terminal region* of dynamic storage modulus G'_b versus dynamic loss modulus G''_b on logarithmic coordinates for the PMMA/PVDF blends, using eq 16 and 17 for $z = 3$,

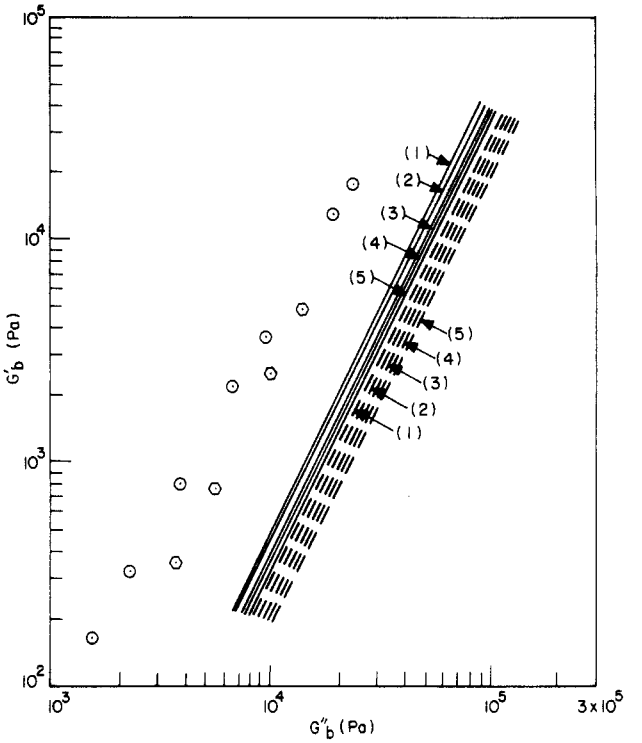

Figure 5. Theoretically predicted log G'_b versus log G''_b plots for PMMA/PVDF blends, consisting of *monodisperse* constituent components, at 230 °C. The solid curves (—) are predicted with eq 16 and 17, and the dashed curves (- - -) are predicted with the 3.4-power blending law together with the reptation contribution only, in the tube model (eq 23 and 24 of ref 1): (1) PVDF; (2) PMMA/PVDF = 20/80; (3) PMMA/PVDF = 40/60; (4) PMMA/PVDF = 60/40; (5) PMMA. Here, $\chi = -0.3$ and $z = 3$ were used for the computations. Symbols represent experimental data:[1] (⊙) PMMA; (⊙) PVDF.

which were derived on the assumption that the constituent components are *monodisperse*. Note that the plots were obtained using the same numerical values for the parameters, which were used to generate the results given in Figure 1. For comparison purposes, the values of log G'_b and log G''_b in the *terminal region*, predicted with the 3.4-power blending law and with reptation contribution only, are also given in Figure 5, where symbols represent experimental data reported in our previous paper.[1] It can be seen in Figure 5 that the theoretical predictions obtained with the linear blending law and with both reptation and constraint release contributions are slightly better than those obtained with the 3.4-power blending law and with reptation contribution only; however, the differences between the predictions for the *monodisperse* constituent components and the experimental results are very large. It should be remembered, however, that the PMMA and PVDF used in the experiment had polydispersities of 2.14 and 2.30, respectively.

Let us now consider the effect of polydispersity of the constituent components on the linear viscoelastic properties of PMMA/PVDF blends. Specifically, values of η_{ob}, $G'_b(\omega)$, and $G''_b(\omega)$ for the binary blends of polydisperse PMMA and PVDF can be calculated, by first determining the relaxation modulus $G_b(t)$ of the blend from

$$G_b(t) = \sum_{i=1}^{n}\left\{\sum_{j=1}^{m}\left[G^\circ_{N1}\frac{\phi_1}{m}w_{1i}\,F_{1i}(t)\,R_{1i}(t) + G^\circ_{N2}\frac{\phi_2}{n}w_{2j}\,F_{2j}(t)\,R_{2j}(t)\right]\right\} \quad (26)$$

where the upper limit n (or m) in the summation notation

denotes the number of fractions, chosen for computational purposes, in the constituent component 1 (or 2), each having the weight fraction w_{1i} (or w_{2j}). It should be noted that when dealing with binary blends having components with *identical* chemical structure (i.e., $\chi = 0$), eq 26 can be rewritten as

$$G_b(t) = G^\circ_{N1}\phi_1[\sum_{i=1}^{n} w_{1i} F_{1i}(t) R_{1i}(t)] + G^\circ_{N2}\phi_2[\sum_{j=1}^{m} w_{2j} F_{2j}(t) R_{2j}(t)] \quad (27)$$

which was used by Graessley and Struglinski.[3]

Note that $F_{1i}(t)$ (or $F_{2j}(t)$) in eq 26 can be calulated by modifying eq 4 (or eq 5); i.e.

$$F_{kl}(t) = \frac{4}{\pi^2}\sum_{p=1}^{\infty}\frac{H_{kl,p}}{p^2}\exp(-p^2 t/\tau_{kl,p}) \quad (28)$$

$$k = 1,\ l = 1, 2, ..., n$$

$$k = 2,\ l = 1, 2, ..., m$$

where $H_{kl,p}$ ($k = 1, 2$) are defined by (see eq 7)

$$H_{kl,p} = \frac{\{1 - (-1)^p \cosh[(-\chi)\phi^*_{kl}Z_{kl}]\}}{\{1 + [(-\chi)\phi^*_{kl}Z_{kl}/p\pi]^2\}^2} \quad (29)$$

$$k = 1,\ l = 1, 2, ..., n$$

$$k = 2,\ l = 1, 2, ..., m$$

in which

$$\phi^*_{1i} = \frac{\phi_2 w_{2j}}{\rho_2}\Big/\left[\frac{\phi_1 w_{1i}}{\rho_1} + \frac{\phi_2 w_{2j}}{\rho_2}\right] \quad (30a)$$

and

$$\phi^*_{2j} = 1 - \phi^*_{1i} \quad (30b)$$

where ρ_1 and ρ_2 are the densities of components 1 and 2, respectively. Also, $\tau_{kl,p}$ ($k = 1, 2$) in eq 28 is defined by (see eq 6)

$$\tau_{kl,p} = \tau'_{dk,l}\Big/\left[1 + \left(\frac{(-\chi)\phi^*_{kl}Z_{kl}}{p\pi}\right)^2\right] \quad (31)$$

$$k = 1,\ l = 1, 2, ..., n$$

$$k = 2,\ l = 1, 2, ..., m$$

where

$$\tau'_{dk,l} = \tau_{dk}(\bar{M}_{w,k})\left(\frac{M_{kl}}{\bar{M}_{w,k}}\right)^{3.4} \quad (32)$$

$$k = 1,\ l = 1, 2, ..., n$$

$$k = 2,\ l = 1, 2, ..., m$$

Note in eq 32 that M_{kl} is greater than the entanglement molecular weight $M_{e,k}$ and that $\tau_{dk}(\bar{M}_{w,k})$ ($k = 1, 2$) can be calculated from τ_{di}, defined by eq 19, with $M = \bar{M}_{w,k}$. Note in eq 32 that an empirical 3.4-power law, $\tau_d \propto M^{3.4}$, was introduced. This is a departure from the prediction of the tube model of Doi and Edwards.[4] The 3.4-power law was used in order to obtain more realistic theoretical predictions, since the molecular weights of PMMA and PVDF used in the PMMA/PVDF blends, and the molecular weights of PMMA and PSAN used in the PMMA/PSAN blends, are greater than the entanglement molecular weights of the respective components.

Values of $R_{kl}(t)$ in eq 26 can be calculated by modifying eq 9; i.e.

$$R_{kl}(t) = \frac{1}{Z_{kl}}\sum_{s=1}^{Z_{kl}}\exp(-\lambda_{s,kl}t/2\tau_w) \quad (33)$$

$$k = 1,\ l = 1, 2, ..., n$$

$$k = 2,\ l = 1, 2, ..., m$$

where

$$\lambda_{s,kl} = 4\sin^2[\pi s/2(Z_{kl} + 1)] \quad (34)$$

The number of segments of component k, Z_{kl}, appearing in eq 33, is given by

$$Z_{kl} = \frac{5}{4}\frac{M_{kl}}{M_{e,k}} \qquad M_{kl} > M_{e,k} \quad (35)$$

and the waiting time τ_w is defined as:

$$\tau_w = \int_0^\infty [\phi_1\sum_{i=1}^{n} w_{1i} F_{1i}(t) + \phi_2\sum_{j=1}^{m} w_{2j} F_{2j}(t)]^z\, dt \quad (36)$$

Assuming $z = 3$, τ_w can be calculated from

$$\tau_w = \left(\frac{4}{\pi^2}\right)^3\sum_i^n\sum_k^n\sum_u^n\sum_j^m\sum_l^m\sum_v^m\left\{\left(\frac{\phi_1}{m}\right)^3 w_{1i}w_{1k}w_{1u}\sum_p^\infty\sum_q^\infty\sum_r^\infty\frac{H_{1i,p}}{p^2}\frac{H_{1k,q}}{q^2}\times\frac{H_{1u,r}}{r^2}\Big/\left[\frac{p^2Q_{1i,p}}{\tau'_{d1,i}} + \frac{q^2Q_{1k,q}}{\tau'_{d1,k}} + \frac{r^2Q_{1u,r}}{\tau'_{d1,u}}\right] + 3\left(\frac{\phi_1^2\phi_2}{nm^2}\right)w_{1i}w_{1k}w_{2v}\sum_p^\infty\sum_q^\infty\sum_r^\infty\frac{H_{1i,p}}{p^2}\frac{H_{1k,q}}{q^2}\frac{H_{2v,r}}{r^2}\Big/\left[\frac{p^2Q_{1i,p}}{\tau'_{d1,i}} + \frac{q^2Q_{1k,q}}{\tau'_{d1,k}} + \frac{r^2Q_{2v,r}}{\tau'_{d2,v}}\right] + 3\left(\frac{\phi_1\phi_2^2}{n^2m}\right)w_{1i}w_{2l}w_{2v}\sum_p^\infty\sum_q^\infty\sum_r^\infty\frac{H_{1i,p}}{p^2}\frac{H_{2l,q}}{q^2}\frac{H_{2v,r}}{r^2}\Big/\left[\frac{p^2Q_{1i,p}}{\tau'_{d1,i}} + \frac{q^2Q_{2l,q}}{\tau'_{d2,l}} + \frac{r^2Q_{2v,r}}{\tau'_{d2,v}}\right] + \left(\frac{\phi_2}{n}\right)^3 w_{2j}w_{2l}w_{2v}\sum_p^\infty\sum_q^\infty\sum_r^\infty\frac{H_{2j,p}}{p^2}\frac{H_{2l,q}}{q^2}\frac{H_{2v,r}}{r^2}\Big/\left[\frac{p^2Q_{2j,p}}{\tau'_{d2,j}} + \frac{q^2Q_{2l,q}}{\tau'_{d2,l}} + \frac{r^2Q_{2v,r}}{\tau'_{d2,v}}\right]\right\} \quad (37)$$

where

$$Q_{kl,p} = 1 + [(-\chi)\phi^*_{kl}Z_{kl}/\pi p]^2 \quad (38)$$

$$k = 1,\ l = 1, 2, ..., n$$

$$k = 2,\ l = 1, 2, ..., m$$

It should be noted that ϕ^*_{1k} in $H_{1k,q}$ and $Q_{1k,q}$ and ϕ^*_{2l} in $H_{2l,q}$ and $Q_{2l,q}$ may be obtained from eq 30, by replacing w_{1i} with w_{1k} and w_{2j} with w_{2l}. Similarly, ϕ^*_{1u} in $H_{1u,r}$ and $Q_{1u,r}$ and ϕ^*_{2v} in $H_{2v,r}$ and $Q_{2v,r}$ may be obtained from eq 30, by replacing w_{1i} with w_{1u} and w_{2j} with w_{2v}.

One can now calculate the η_{ob} of binary blends consisting of two *polydisperse* components from the following expression

$$\eta_{ob} = \int_0^\infty G_b(t)\, dt \quad (39)$$

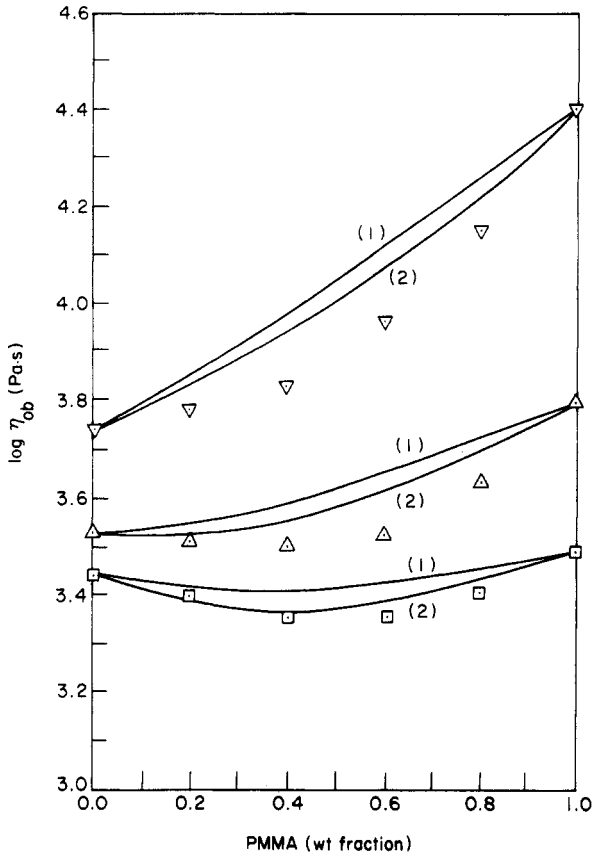

Figure 6. Theoretically predicted log η_{ob} versus blend composition plots for PMMA/PVDF blends. Here $\chi = -0.3$ and $z = 3$ were used in the computations. Curve (1) is predicted for *monodisperse* PMMA and PVDF using eq 22, and curve (2) is predicted for *polydisperse* PMMA and PVDF using eq 39, together with eq 26 and eq 28 through eq 38 where the polydispersity ($\bar{M}_w/\bar{M}_n$) is 2.14 for PMMA and 2.31 for PVDF. Symbols represent experimental data[1] at different temperatures (°C): (▽) 200; (△) 220; (□) 230.

where $G_b(t)$ was defined by eq 26. In the present study, we calculated values of η_{ob} for PMMA/PVDF blends, with the polydispersity of PMMA equal to 2.14 and polydispersity of PVDF equal to 2.30, by assuming that the molecular weight distribution of PMMA and PVDF is each represented by a log-normal distribution function. The results are given in Figure 6. Due to the very large computational time required for obtaining τ_w defined by eq 37, we used a total of six fractions for each component (i.e., $n = m = 6$) and $p = q = r = 20$ appearing in eq 37. It can be seen from Figure 6 that the inclusion of the polydispersities of the constituent components into the calculation brings theoretical predictions closer to experimental results, but a better agreement between the two is desirable. When discussing the results given in Figure 1, we already pointed out the directions that should be taken for improving the present theory.

Due to the very large computational times required, we only calculated values of $G'_b(\omega)$ and $G''_b(\omega)$ for polydisperse PMMA and PVDF separately and not for binary blends consisting of polydisperse PMMA and PVDF. In this case, substitution of $m = 1$ and $\phi_2 = 0$ in eq 26 (or $\phi_2 = 0$ in eq 27) gives the expression for $G_b(t)$. For this we used the following expressions for $F_i(t)$ for PMMA and PVDF, respectively

$$F_i(t) = \frac{8}{\pi^2} \sum_{\substack{p=1 \\ \text{odd}}}^{\infty} \frac{1}{p^2} \exp(-p^2 t/\tau'_{di}) \qquad i = 1, 2, ..., n \tag{40}$$

and for τ_w

$$\tau_w = \left(\frac{8}{\pi^2}\right)^3 \sum_{i}^{n}\sum_{k}^{n}\sum_{u}^{n} w_i w_k w_u \sum_{\substack{p \\ \text{all}}}^{\infty}\sum_{\substack{q \\ \text{odd}}}^{\infty}\sum_{\substack{r \\ \text{odd}}}^{\infty} \frac{1}{p^2}\frac{1}{q^2}\frac{1}{r^2} \Bigg/ \left[\frac{p^2}{\tau'_{d,i}} + \frac{q^2}{\tau'_{d,k}} + \frac{r^2}{\tau'_{d,u}}\right] \tag{41}$$

Figure 7 gives theoretically predicted plots of G'_b versus G''_b in the *linear* region for *polydisperse* PMMA and PVDF, obtained with the linear blending law together with both reptation and constraint release contributions in the tube model. In obtaining the results given in Figure 7, we used 10 fractions ($n = 10$) in the log-normal distribution function for molecular weights greater than M_e. For comparison purposes, the predictions obtained with the 3.4-power blending law together with reptation contribution only are also given in Figure 7. A comparison of Figure 7 with Figure 5 reveals that (1) the predictions of G'_b and G''_b obtained for *polydisperse* PMMA and PVDF are much better than those obtained for *monodisperse* PMMA and PVDF and (2) the slope of log G'_b versus log G''_b plots decreases with increasing polydispersity. Using the tube model with both reptation and constraint release contributions, it is shown in the Appendix that the slope of log G'_b versus log G''_b plots decreases from 2 (for monodisperse homopolymers) with increasing polydispersity and that the polydispersity of the polymer shifts the log G'_b versus log G''_b plots upward, the extent of which depends on the degree of polydispersity. Figure 7 shows further that the predictions of G'_b and G''_b obtained with the linear blending law together with both reptation and constraint release contributions for $z = 3$ in the tube model are much better than those obtained with the 3.4-power blending law together with reptation contribution only.

Very recently, Wu[13,14] reported the results of measurements of the plateau modulus of compatible blends, G°_{Nb}, namely, PMMA/PVDF and PMMA/PSAN blend systems, and showed that plots of G°_{Nb} versus blend composition exhibit *negative* deviations from linearity for *both* blend systems investigated. He used an empirical, quadratic expression to fit his experimental data.

We will now derive theoretical expressions for G°_{Nb} for compatible polymer blends, using the theory presented above. For this, let us assume that G°_{Nb} can be determined from the expression

$$G^\circ_{Nb} = [G_b(t)]_{t=\tau_e} \tag{42}$$

where $G_b(t)$ is the relaxation modulus of the blend and τ_e is the Rouse relaxation time for a polymer chain between two adjacent entanglement points. Note that τ_e is independent of molecular weight and that the values of τ_e are smaller than the values of the Rouse relaxation time, τ_r, for the primitive chain and also much smaller than the values of the tube disengagement time, τ_d (i.e., $\tau_e < \tau_r < \tau_d$). For the linear blending law defined by eq 8, we have

$$G^\circ_{Nb} = w_1 G^\circ_{N1} F_1(\tau_e) R_1(\tau_e) + w_2 G^\circ_{N2} F_2(\tau_e) R_2(\tau_e) \tag{43}$$

where $F_i(t)$ and $R_i(t)$ are defined by eq 4, 5, and 9. It can be shown that[15]

$$F_i(\tau_e) = \frac{4}{\pi} \sum_{p=1}^{\infty} \frac{H_{i,p}}{p^2} \simeq 1 \tag{44}$$

$$R_i(\tau_e) \simeq 1 \tag{45}$$

From eq 43–45 we then obtain

$$G^\circ_{Nb} = w_1 G^\circ_{N1} + w_2 G^\circ_{N2} \tag{46}$$

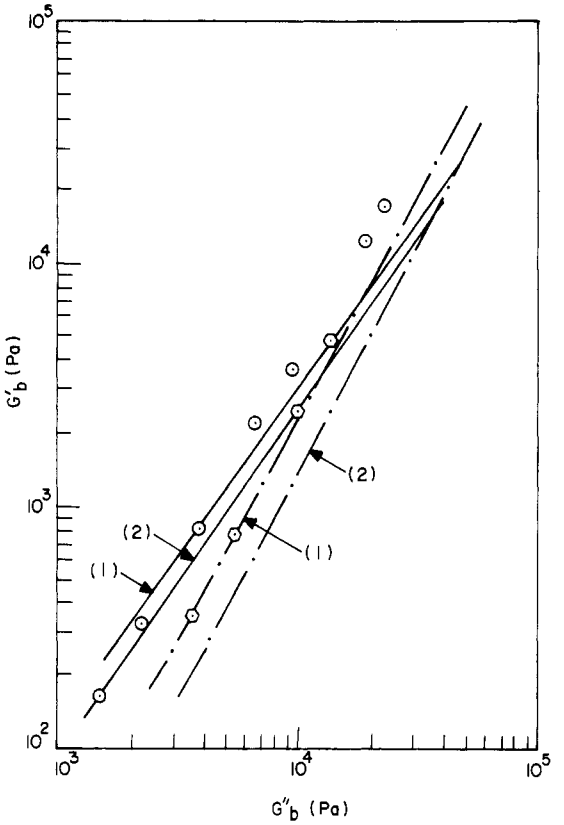

Figure 7. Theoretically predicted log G'_b versus log G''_b plots for *polydisperse* PMMA and PVDF at 230 °C, whose molecular weight distributions are represented by the log-normal distribution function. Here $\chi = -0.3$ and $z = 3$ were used in the computations. The polydispersity ($\bar{M}_w/\bar{M}_n$) is 2.14 for PMMA and 2.31 for PVDF. The solid curves (—) were obtained with the linear blending law with both the reptation and constraint release contributions, in the tube model, and the broken curves (-·-) were obtained with the 3.4-power blending law together with the reptation contribution only, in the tube model. Symbols represent the experimental data:[1] (⊙) PMMA; (⊙) PVDF. Curve (1) is for PVDF, and curve (2) is for PMMA.

Figure 8 displays the predictions of G°_{Nb} for PMMA/PVDF blends based on eq 46 together with the experimental data of Wu,[13] and Figure 9 gives similar plots for PMMA/PSAN blends. It can be seen from both Figures 8 and 9 that eq 46 predicts a linear relationship between G°_{Nb} and blend composition, which is far removed from experimental observations.

If the 3.4-power blending law for the relaxation modulus is used and only the reptation contribution is included in the tube model, we can derived from eq 42, with the aid of eq 44 and 45, the following expression for G°_{Nb}:

$$G^\circ_{Nb} = [w_1(G^\circ_{N1})^{1/3.4} + w_2(G^\circ_{N2})^{1/3.4}]^{3.4} \qquad (47)$$

For comparison purposes, the predictions of G°_{Nb} obtained with eq 47 are also given in Figure 8 for PMMA/PVDF blends and in Figure 9 for PMMA/PSAN blends. It can be seen in Figures 8 and 9 that eq 47 predicts *negative* deviations of G°_{Nb} from linearity, which are consistent with experimental observations, but further improvement is needed. It should be remembered that when plotted against blend composition, the blend viscosity η_{ob} exhibits *negative* deviations from linearity for PMMA/PVDF blends and *positive* deviations from linearity for PMMA/PSAN blends (see Figures 1 and 2). We have attributed this discrepancy to the difference in the values of the interaction parameter χ between PMMA/PVDF blends and PMMA/PSAN blends. Interestingly enough, however, the experimental data of Wu[13,14] appears to

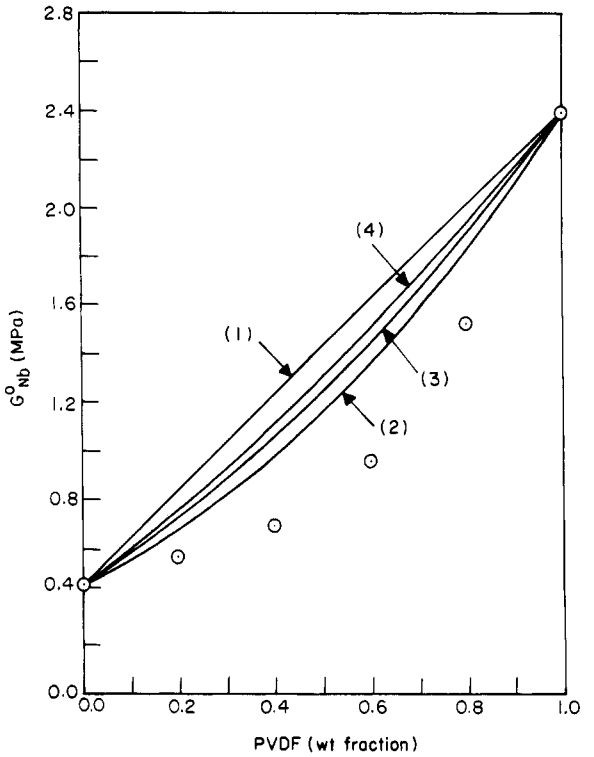

Figure 8. Comparison of theoretical predictions with experimental results for the dependence of G°_{Nb} on blend composition for PMMA/PVDF blends. Curve (1) represents predictions made with eq 46; curve (2) represents predictions made with eq 47; curve (3) represents predictions made with eq 48; curve (4) represents predictions made with eq 50. The symbol (⊙) represents experimental data.[13]

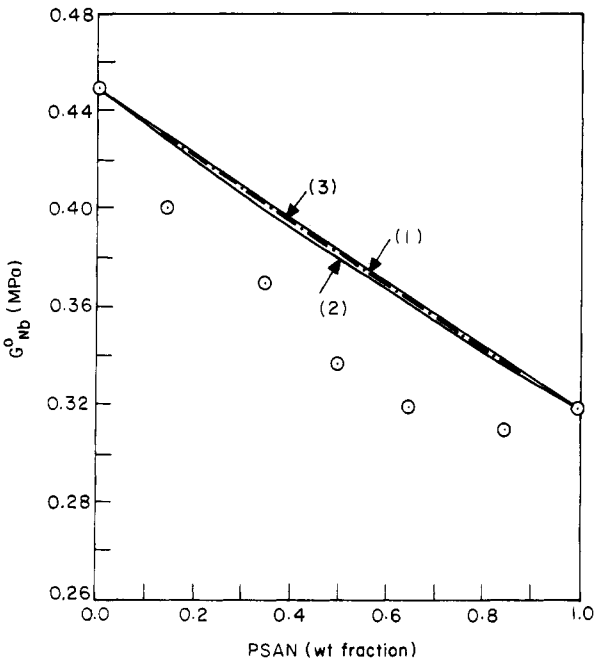

Figure 9. Comparison of theoretical predictions with experimental results for the dependence of G°_{Nb} on blend composition for PMMA/PSAN blends. Solid curve (1) represents predictions made with eq 46; solid curve (2) represents predictions made with eq 47; broken curve (3) represents predictions made with eq 48. The symbol (⊙) represents experimental data.[14]

suggest that the plateau modulus of compatible polymer blends is not sensitive to values of the interaction parameter χ. This indeed is predicted by eq 47.

It seems appropriate to mention at this juncture some of the earlier attempts made to correlate the plateau mo-

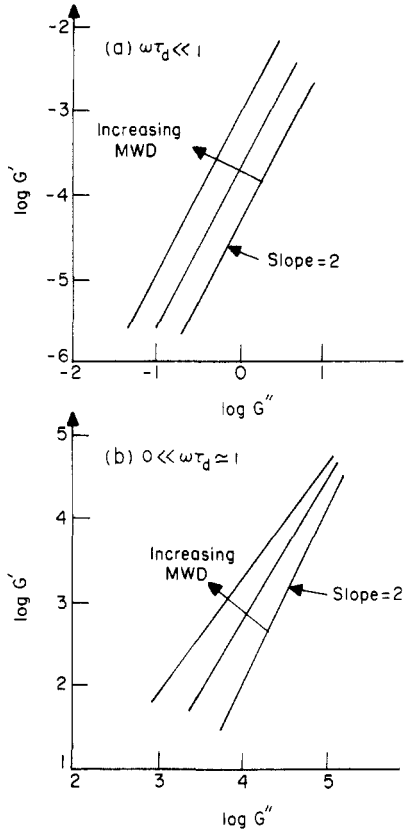

Figure 10. Schematic representation of the dependence of log G' versus log G'' plots on polydispersity: (a) in the terminal region; (b) in the linear region.

dulus of polymer blends with composition. Very recently, Composto[9] derived the expression

$$G^\circ_{Nb} = [\phi_1(G^\circ_{N1})^{1/2} + \phi_2(G^\circ_{N2})^{1/2}]^2 \quad (48)$$

for the plateau modulus of blends of poly(2,6-dimethyl-1,4-phenylene oxide) and polsytyrene, based on a scaling law developed by Graessley and Edwards.[16] In the derivation of eq 48, Composto assumed that the Kuhn statistical lengths of the constituent components were the same and then applied eq 48 to calculate the plateau modulus for blends of polystyrene and poly(2,6-dimethyl-1,4-phenylene oxide). He obtained reasonably good agreement between predictions and experimental results for the particular blend system considered. Tsenoglou[17] also derived, independently, eq 48.

Since the Kuhn statistical lengths of PMMA (l_1 = 64.0 nm) and PVDF (l_2 = 52.2 nm) are different, we must use an expression that is more general than eq 48. If the Kuhn statistical length l_b for a binary blend is assumed to be given by

$$l_b^2 = \phi_1 l_1^2 + \phi_2 l_2^2 \quad (49)$$

we can obtain

$$G^\circ_{Nb} = \left[\phi_1 + \phi_2\left(\frac{l_2}{l_1}\right)^2\right]^{1/2}\left[\phi_1(G^\circ_{N1})^{1/2} + \phi_2(G^\circ_{N2})^{1/2}\left(\frac{l_1}{l_2}\right)^{1/2}\right]^2 \quad (50)$$

The values of G°_{Nb} for the PMMA/PVDF blend system, predicted with eq 48 and 50, are given in Figure 8, in which weight fractions, instead of volume fractions, were used. Similar results are given in Figure 9 for the PMMA/PSAN blend system. It can be seen in Figure 8 that the theoretical predictions made by the quadratic expression, eq 48 or 50, lie between those made by the linear blending law, eq 46, and those made by the 3.4-power blending law, eq 47. When other expressions, $l_b = \phi_1 l_1 + \phi_2 l_2$ and $1/l_b = \phi_1/l_1 + \phi_2/l_2$, respectively, were used, we obtained results that deviate within 10% from those predicted with eq 48.

Wu[13,14] used the following expression for the plateau modulus of binary blends

$$G^\circ_{Nb} = \phi_1^2 G^\circ_{N1} + \phi_2^2 G^\circ_{N2} + 2\phi_1\phi_2 RT(\rho_1\rho_2)^{1/2}/M^\circ_{e12} \quad (51)$$

and calculated values of G°_{Nb} for PMMA/PVDF and PMMA/PSAN blends, respectively. In eq 51, R is the universal gas constant, T is the absolute temperature, ρ_1 and ρ_2 are the densities of components 1 and 2, respectively, and M°_{e12} is a hypothetical entanglement molecular weight of the blend. In correlating his experimental data, Wu used M°_{e12} as an adjustable parameter.

Equation 48 can be rewritten in the following form:

$$G^\circ_{Nb} = \phi_1^2 G^\circ_{N1} + \phi_2^2 G^\circ_{N2} + 2\phi_1\phi_2(G^\circ_{N1}G^\circ_{N2})^{1/2} \quad (52)$$

It can be seen that eq 51 reduces to eq 52 if the following relationship holds:

$$M^\circ_{e12} = (M^\circ_{e1}M^\circ_{e2})^{1/2} \quad (53)$$

According to Composto,[9] eq 52 predicts reasonably well the values of G°_{Nb} for blends of polystyrene and poly(2,6-dimethyl-1,4-phenylene oxide). In such a case, M°_{e12} can be calculated using eq 53. However, in general, eq 53 may not hold for binary blends consisting of components with *dissimilar* chemical structures (e.g., PMMA/PVDF and PMMA/PSAN blend systems).

Equation 52 can be generalized to obtain an expression for the relaxation modulus $G_b(t)$ of binary blends

$$G_b(t) = \phi_1^2 G_1(t) + \phi_2^2 G_2(t) + 2\phi_1\phi_2 G_{12}(t) \quad (54)$$

where

$$G_1(t) = G^\circ_{N1}F_1(t/\tau_1) \quad (55a)$$

$$G_2(t) = G^\circ_{N2}F_2(t/\tau_2) \quad (55b)$$

$$G_{12}(t) = G^\circ_{N12}F_{12}(t/\tau_{12}) \quad (55c)$$

Note that eq 54 reduces to eq 52 for $t = 0$. Using eq 54 in eq 39, we can now obtain the following expression for blend viscosity η_{ob}:

$$\eta_{ob} = \phi_1^2\eta_{o1} + \phi_2^2\eta_{o2} + 2\phi_1\phi_2\eta_{o12} \quad (56)$$

In correlating his experimental data, Wu[18] used the expression

$$\log \eta_{ob} = \phi_1^2 \log \eta_{o1} + \phi_2^2 \log \eta_{o2} + 2\phi_1\phi_2 \log \eta_{o12} \quad (57)$$

for blend viscosity and adjusted the value of η_{o12} to give the best fit to experimental data. It should be pointed out that eq 56 is derived from eq 54, whereas eq 57 cannot be derived from eq 51. Thus, one can conclude that there is *no* internal consistency between eq 51 and 57, and thus eq 57 must be regarded as an empirical expression.

4. Concluding Remarks

We have extended our previous study[1] to develop a molecular theory, which predicts the zero-shear viscosity, η_{ob}, steady-state compliance, J°_{eb}, dynamic storage modulus, $G'_b(\omega)$, and dynamic loss modulus, $G''(\omega)$, for compatible polymer mixtures, by including both the reptation and constraint release contributions in the tube model. In the development of the theory, it is assumed that each primitive chain reptates in a separate tube, but molecular

interactions between the two chemically *dissimilar* primitive chains take place under the influence of an external potential defined by eq 2, and that the constraint release contribution is represented by eq 9–11. The external potential is assumed to be dependent upon the interaction parameter χ of the constituent components. By assuming a linear blending law for the relaxation modulus $G_b(t)$, we have obtained expressions for η_{ob}, $G'_b(\omega)$, $G''_b(\omega)$, and J°_{eb} for binary mixtures of compatible polymers. The theoretical predictions compared favorably with experimental data. We have shown that the interaction parameter χ plays a central role in determining the shape of the η_{ob} versus blend composition curve for compatible polymer mixtures and that polydispersity has a profound influence on the elastic properties (i.e., dynamic storage modulus, $G_b'(\omega)$, in the present study) of a polymer.

It should be mentioned, in reference to Figures 5 and 7, that (a) we have not included separate plots for different temperatures since log G' versus log G'' plots are *very* weak functions of temperature (or *virtually* independent of temperature)[19-21] and, (b) due to the very long computational times required, we carried out computations to study the effect of polydispersity on log G'_b versus log G''_b plots only for the homopolymers, PMMA and PVDF.

The inclusion of the constraint release contribution in the tube model developed in our previous paper,[1] together with the linear blending law for the relaxation modulus, has enabled us to obtain *exact* analytical expressions for η_{ob}, $G'_b(\omega)$, and $G''_b(\omega)$ for compatible polymer blends. Note that the 3.4-power blending law for the relaxation modulus does not allow us to obtain *exact* analytical expressions for η_{ob}, $G'_b(\omega)$, and $G''_b(\omega)$, and thus only *approximate* analytical expressions were obtained.[1] The present study shows that (1) the predictions of η_{ob} obtained with the linear blending law together with reptation and constraint release contributions, for $z = 3$, in the tube model are more or less the same as those obtained with the 3.4-power blending law together with the reptation contribution only and (2) the predictions of G°_{Nb} are much better with the 3.4-power blending law together with the reptation contribution only in the tube model than with the linear blending law together with the reptation and constraint release contributions.

Using the tube model concept, we have developed expressions for the plateau modulus of compatible polymer blends, G°_{Nb}, as functions of blend composition and found that the linear blending law and reptation and constraint release contributions in the tube model predict a linear relationship between G°_{Nb} and blend composition, whereas the 3.4-power blending law and reptation contribution only predicts *negative* deviations of G°_{Nb} from linearity, when plotted against blend composition, which is consistent with experimental observations. Further study is needed to develop a blending law that will give satisfactory predictions of η_{ob}, $G'_b(\omega)$, $G''_b(\omega)$, and G°_{Nb} for compatible polymer blends.

Appendix

In order to observe the effect of polydispersity of a homopolymer on the slope of log G'_b versus log G''_b plots, let us assume that the relaxation modulus of a blend $G_b(t)$ can be represented by eq 27 with $\phi_2 = 0$. Using $F_i(t)$ defined by eq 40 and $R_i(t)$ defined by eq 33 in eq 27, the dynamic storage modulus, $G'_b(\omega)$, and loss modulus, $G''_b(\omega)$, respectively, for *polydisperse* polymers can be written as

$$G'_b(\omega) = \frac{8G^\circ_N}{\pi^2}\sum_{i=1}^{n}\left[\sum_{\substack{\text{odd}\\p}}^{\infty}\frac{1}{p^2}\frac{1}{Z_i}\sum_{j=1}^{Z_i}\frac{(\omega\tau_{di,j})^2}{1+(\omega\tau_{di,j})^2}\right]\phi_i(Z_i) \quad \text{(A1)}$$

and

$$G''_b(\omega) = \frac{8G^\circ_N}{\pi^2}\sum_{i=1}^{n}\left[\sum_{\substack{\text{odd}\\p}}^{\infty}\frac{1}{p^2}\frac{1}{Z_i}\sum_{j=1}^{Z_i}\frac{\omega\tau_{di,j}}{1+(\omega\tau_{di,j})^2}\right]\phi_i(Z_i) \quad \text{(A2)}$$

where n is the number of the fractions (to be specified for the computation) in a polydisperse polymer, Z_i is the number of steps along the primitive path, $\phi_i(Z_i)$ is the fractional weight of the polymer with path steps in the range between Z_i and $Z_i + dZ_i$, and $\tau_{di,j}$ is defined by

$$1/\tau_{di,j} = p^2/\tau'_{di} + \lambda_{j,i}/2\tau_w \quad \text{(A3)}$$

where τ'_{di} is defined by eq 32, $\lambda_{j,i}$ by eq 34, and τ_w by eq 41.

In the *terminal* region, where $\omega\tau_{di,j} \ll 1$, for large values of Z_i eq A1 and A2 reduce to

$$\log G'_b = 2\log G''_b + \frac{\pi^2}{16}\frac{1}{G^\circ_N}\sum_{i=1}^{n}\phi_i\sum_{\substack{\text{odd}\\p}}^{\infty}\frac{\tau_{di}^2}{p^5}\frac{2p^2+r_i}{(p^2+r_i)^{3/2}}\Bigg/\left[\sum_{i=1}^{n}\phi_i\sum_{\substack{\text{odd}\\p}}^{\infty}\frac{1}{p^3}\frac{\tau_{di}}{(p^2+r_i)^{1/2}}\right]^2 \quad \text{(A4)}$$

where $r_i = 2\tau'_{di}/\tau_w$ ($i = 1, 2, ..., n$). Note that for *monodisperse* polymers eq A4 reduces to

$$\log G' = 2\log G'' + \frac{\pi^2}{16}\frac{1}{G^\circ_N}\sum_{\substack{\text{odd}\\p}}^{\infty}\frac{1}{p^5}\frac{2p^2+r}{(p^2+r)^{3/2}}\Bigg/\left[\sum_{\substack{\text{odd}\\p}}^{\infty}\frac{1}{p^3}\frac{1}{(p^2+r)^{1/2}}\right]^2 \quad \text{(A5)}$$

where $r = 2\tau_d(M)/\tau_w$. A comparison of eq A4 with eq A5 indicates that, in the *terminal* region, log G'_b versus log G''_b plots for *polydisperse* polymers will have a slope of 2, with the values of G'_b shifted upward above the values of G' in the log G' versus log G'' plots for *monodisperse* polymers, the extent of the shift being greater with increasing polydispersity. Figure 10 shows schematically how polydispersity affects the shape of log G' versus log G'' plots, namely: (a) in the terminal region where $\omega\tau_d \ll 1$, the slope of log G' versus log G'' plots is 2 for both monodisperse polymers and their blends (i.e., polydisperse polymers), but an increase in the polydispersity of a polymer shifts the values of G' to higher values in the log G' versus log G'' plots; (b) in the linear region where $0 \ll \omega\tau_d \approx 1$, the slope of the log G' versus log G'' plots decreases steadily from the value of 2, with increasing polydispersity for polydisperse polymers.

In the *linear* region, where $0 \ll \omega\tau_d \approx 1$ holds, the denominators in eq A1 and A2 are no longer negligible. In order to facilitate mathematical operations, without loss of generality, we will consider a single relaxation time in the relaxation modulus. For *polydisperse* polymers, eq A1 and A2, respectively, with $p = 1$ reduce to

$$\log G'_b(\omega) = \log\left(\frac{8G^\circ_N}{\pi^2}\right) + \log\left(\sum_{i=1}^{n}\frac{\phi_i}{Z_i}\sum_{j=1}^{Z_i}\frac{(\omega\tau_{i,j})^2}{1+(\omega\tau_{i,j})^2}\right) \quad \text{(A6)}$$

and

$$y\log G''_b(\omega) = y\log\left(\frac{8G^\circ_N}{\pi^2}\right) + \log\left(\sum_{i=1}^{n}\frac{\phi_i}{Z_i}\sum_{j=1}^{Z_i}\frac{\omega\tau_{i,j}}{1+(\omega\tau_{i,j})^2}\right)^y \quad \text{(A7)}$$

where y is a real number greater than zero and

$$1/\tau_{i,j} = 1/\tau'_{di} + \lambda_j/2\tau_w \quad \text{(A8)}$$

Multiplying the argument of the last term in eq A6 by $\sum_{i=1}^{n}\phi_i = 1$, we obtain

$$\sum_{i=1}^{n}\frac{\phi_i^2}{Z_i}\sum_{j=1}^{Z_i}\frac{(\omega\tau_{i,j})^2}{1+(\omega\tau_{i,j})^2} + \sum_{\substack{i,k\\k\neq i\\k>i}}^{n}\phi_i\phi_k\left[\frac{1}{Z_i}\sum_{j=1}^{Z_i}\frac{(\omega\tau_{i,j})^2}{1+(\omega\tau_{i,j})^2} + \frac{1}{Z_k}\sum_{j=1}^{Z_k}\frac{(\omega\tau_{k,j})^2}{1+(\omega\tau_{k,j})^2}\right] \quad \text{(A9)}$$

Similarly, the argument of the last term in eq A7 for $y = 2$ becomes

$$\sum_{i=1}^{n}\phi_i^2\left(\frac{1}{Z_i}\sum_{j=1}^{Z_i}\frac{\omega\tau_{i,j}}{1+(\omega\tau_{i,j})^2}\right)^2 + 2\sum_{\substack{i,k\\k\neq i\\k>i}}^{n}\phi_i\phi_k\left\{\left[\frac{1}{Z_i}\sum_{j=1}^{Z_i}\frac{\omega\tau_{i,j}}{1+(\omega\tau_{i,j})^2}\right]\left[\frac{1}{Z_k}\sum_{j=1}^{Z_k}\frac{\omega\tau_{k,j}}{1+(\omega\tau_{k,j})^2}\right]\right\} \quad \text{(A10)}$$

When inequality relationships are used, it can be shown that the magnitude of eq A9 is greater than that of eq A10; therefore, the magnitude of the last term in eq A6 must be greater than that of the last term in eq A7, for $y = 2$.

In view of the fact that, for $\omega\tau_{i,j} < 1$, $(\omega\tau_{i,j})^2 < \omega\tau_{i,j} \approx 1$ and thus the magnitude of eq A9 is greater than that of eq A10, there must exist a value of x, greater than 1 but less than 2, that satisfies the following equality:

$$\sum_{i=1}^{n}\frac{\phi_i}{Z_i}\sum_{j=1}^{Z_i}\frac{(\omega\tau_{i,j})^2}{1+(\omega\tau_{i,j})^2} = \left(\sum_{i=1}^{n}\frac{\phi_i}{Z_i}\sum_{j=1}^{Z_i}\frac{\omega\tau_{i,j}}{1+(\omega\tau_{i,j})^2}\right)^x \quad \text{(A11)}$$

For a value of x that satisfies equality A11, eq A6 and A7 give

$$\log G'_b = x \log G''_b + (1-x)\log(8G^\circ_N/\pi^2) \quad \text{(A12)}$$

Since the value of x satisfies the inequality $1 < x < 2$, it can be concluded from eq A12, that, in the *linear* region, the slope of $\log G'_b$ versus $\log G''_b$ plots is less than 2 for *polydisperse* polymers. Note that for *monodisperse* polymers eq A12 reduces to

$$\log G' = 2\log G' + \log(\pi^2/8G^\circ_N) \quad \text{(A13)}$$

which was considered previously.[20,21] The above analysis can be extended to any number of relaxation times ($p = 1, 2, \ldots, N$).

Registry No. PMMA, 9011-14-7; PVDF, 24937-79-9; PSAN, 9003-54-7.

References and Notes

(1) Han, C. D.; Kim, J. K. *Macromolecules* **1989**, *22*, 1914.
(2) Graessley, W. W. *Adv. Polym. Sci.* **1982**, *47*, 67.
(3) Graessley, W. W.; Struglinski, M. J. *Macromolecules* **1986**, *19*, 1754.
(4) Doi, M.; Edwards, S. F. *J. Chem. Soc., Faraday Trans. 2* **1978**, *74*, 1789, 1802, 1818.
(5) Struglinski, M. J. Viscoelastic Effects of Polydispersity Studied with Mixtures of Different Chain Architectures. Doctoral Dissertation, Northwestern University, Evanston, IL, 1984.
(6) The right-hand side of eq 27 in ref 3 must be multiplied by $^1/_2$.
(7) Nishi, T.; Wang, T. T. *Macromolecules* **1975**, *8*, 909.
(8) Schmitt, B. J.; Kirste, R. G.; Jelenic, J. *Macromol. Chem.* **1980**, *181*, 1655.
(9) Composto, R. J. Diffusion in Polymer Blends. Doctoral Dissertation, Cornell University, Ithaca, NY, 1987.
(10) Montfort, J. P.; Marin, G.; Monge, Ph. *Macromolecules* **1986**, *19*, 1979.
(11) Struglinski, M. J.; Graessley, W. W. *Macromolecules* **1985**, *18*, 2630.
(12) Lifshitz, E. M.; Pitaevskii, L. P. *Statistical Physics*, 3rd Ed.; Pergamon Press: Oxford, 1980; Part 1, p 377.
(13) Wu, S. *J. Polym. Sci. Part B: Polym. Phys.* **1987**, *25*, 557.
(14) Wu, S. *Polymer* **1987**, *28*, 1144.
(15) Note that $\sum_{p=1}^{\infty}[1-(-1)^p\cosh\theta_i]/p^2[1+(\theta_i/p\pi)^2]^2$ approaches $\pi^2/4$ for values of $\theta_i \leq 50$, where $\theta_i = (-\chi)\phi^*_i Z_i$. For the PMMA/PVDF and PMMA/PSAN blend systems under consideration in this study, values of θ_i are less than 10.
(16) Graessley, W. W.; Edwards, S. F. *Polymer* **1981**, *22*, 1329.
(17) Tsenoglou, C. *ACS Polym. Prepr.* (a) **1987**, *28*(2), 185, 187; (b) **1988**, *29*(1), 405.
(18) Wu, S. *J. Polym. Sci., Part B: Polym. Phys.* **1987**, *25*, 2511.
(19) (a) Han, C. D.; Chuang, H. K. *J. Appl. Polym. Sci.* **1985**, *30*, 2431. (b) Chuang, H. K.; Han, C. D. *J. Appl. Polym. Sci.* **1984**, *29*, 2205. (c) Han, C. D.; Yang, H. H. *J. Appl. Polym. Sci.* **1987**, *33*, 1199.
(20) Han, C. D.; Jhon, M. S. *J. Appl. Polym. Sci.* **1986**, *32*, 3809.
(21) Han, C. D. *J. Appl. Polym. Sci.* **1988**, *35*, 167.